THE ASTROPHYSICAL JOURNAL, 565:645–647, 2002 January 20

ELECTRON EXCITATION CROSS SECTIONS FOR THE $2s^2 2p^2\ ^3P \rightarrow 2s^2 2p^2\ ^1D$ TRANSITION IN O^{2+}

M. NIIMURA, S. J. SMITH, AND A. CHUTJIAN
Atomic and Molecular Collisions Team Jet Propulsion Laboratory, California Institute of Technology, 4800 Oak Grove Drive, Pasadena, CA 901109
Received 2001 April 6; accepted 2001 September 18

ABSTRACT

Absolute experimental excitation cross sections are reported for the combined $2s^2 2p^2\ ^3P_{0,1,2} \rightarrow 2s^2 2p^2\ ^1D_2$ spin- and symmetry-forbidden transitions in O^{2+}. These excitations correspond to the optical emission wavelengths λ5009.0 ($J = 2 \rightarrow 2$) and λ4960.9 ($J = 2 \rightarrow 1$). Use is made in the measurements of the electron energy-loss method with merged electron and ion beams. Data are reported for the center-of-mass collision energy range of 2.48 eV (threshold) to 5.35 eV (or 2.2× threshold). One finds agreement between experiment and some of the predictions of resonances in a recent 26 state ***R***-matrix calculation. In particular, experiment confirms the presence of strong, narrow resonances near 2.7 and 4.2 eV, detectable with an experimental electron-beam energy spread of only 0.10 eV (FWHM). Resonance enhancement predicted at 3.1 eV is absent in the experiment.

Subject headings: atomic data — atomic processes

1. INTRODUCTION

Transitions in the O^{2+} ion are detected in a variety of astrophysical objects such as our own Sun (Doschek et al. 1999), diffuse nebulae-H II regions (Pilyugin 2000), planetary nebulae (Beer & Vaughan 1999; Gorny et al. 1999), and the Io torus (Herbert & Hall 1998; Küppers & Jockers 1997). The strength of the $\lambda\lambda$4960.9, 5009.0 lines (Bashkin & Stoner 1975; also sometimes cited as the $\lambda\lambda$4960, 5007 lines) depends on the brightness of the illuminating central stars, as well as on electron temperature (T_e) and number density (N_e) (Crawford et al. 2000). In order to convert the measured line intensities to actual T_e and N_e one needs reliable experimental measurements, or accurate theoretical data (Crawford et al. 2000; Aggarwal & Keenan 1999). For almost all ionic species, and for practically all charge states and transitions, only theoretical data are available, with no comparison to absolute, or even normalized, experimental cross sections. Presented herein are the first experimental measurements of absolute collisional excitation cross sections for the $2s^2 2p^2\ ^3P \rightarrow 2s^2 2p^2\ ^1D_2$ transitions ($\lambda\lambda$4960.9, 5009.0) in O^{2+}. As part of the JPL effort to establish "ground truth" for theory, comparison is made with the recent 26 state ***R***-matrix calculation of Aggarwal & Keenan (1999) for this transition.

2. EXPERIMENTAL METHODS

The experimental measurements were carried out at JPL using the 14.0 GHz electron cyclotron resonance ion source (ECRIS) (Chutjian et al. 1999; Greenwood et al. 1999; Lozano et al. 2001). Only the different experimental conditions will be discussed here. The O^{2+} was generated from CO feed gas, and extracted at 2 × 6.4 keV from the ECRIS. The metastable fraction in the O^{2+} beam was determined from the gas attenuation technique (Smith et al. 1996; Greenwood, Chutjian, & Smith 2000). The fraction was found to vary between 5% and 25% for the different daily ECRIS running conditions and was applied to the measured cross sections. All other procedures, such as measurements of the electron and ion beams overlap, use of retarding grids and the electrostatic aperture to discriminate against elastically scattered electrons, and correction at higher energies for the residual overlap between high-angle elastically scattered electrons and low-angle inelastically scattered electrons were the same as described in Smith et al. (2000).

In order to convert a signal rate to an absolute cross section, one needs to measure a number of experimental parameters. The relation between these measured quantities and the excitation cross section $\sigma(E)$ (cm^2) at a center-of-mass (CM) energy E is given by

$$\sigma(E) = \frac{\Re q e^2 \Im}{\epsilon I_i I_e L} \left| \frac{v_e v_i}{v_e - v_i} \right| , \qquad (1)$$

where $\Re$ is the total signal rate (s^{-1}), q is the ionic charge state, e is the electron charge (C), I_e and I_i are the electron and ion beam currents (A) respectively, v_e and v_i are the electron and ion velocities (cm s^{-1}), respectively, L is the merged path length (cm), ε is the efficiency of the rejection grids/microchannel-plate detection system (dimensionless), and $\Im$ is the overlap factor between the electron and ion beams (cm^2). All quantities in equation (1) are measured, except for the particle velocities, which are known nominally through their extraction potentials.

3. RESULTS AND DISCUSSION

Results of theoretical calculations for these transitions are available from a 26 LS-coupled target state, ***R***-matrix calculation (Aggarwal & Keenan 1999; see also Aggarwal 1993). These calculations included the $1s^2$, $2s^2 2p^2$, $2s 2p^3$, $2p^4$, $2s^2 2p 3s$, $2s^2 2p 3p$, and $2s^2 2p 3d$ configurations in O III. The target states were constructed from configuration-interaction (CI) wavefunctions using the $1s$, $2s$, and $2p$ Hartree-Fock (HF) orbitals; and $\overline{3s}$, $\overline{3p}$, $\overline{3d}$, $\overline{4s}$, $\overline{4p}$, and $\overline{4d}$ pseudo-orbitals. Radial parameters for the HF calculation were taken from Clementi & Roetti (1974), and those for the pseudo-orbitals from the CIV3 program of Hibbert (1975). All partial waves of angular momentum $L \leq 40$ were included. Relativistic effects were not included for this low charge-state ion. Further details are given in Aggarwal & Keenan (1999).

Results of the 26 state calculation are shown by the solid line in Figure 1. These cross sections were obtained from the collision strengths in LSJ coupling provided by Aggarwal & Keenan (1999). Supplemental collision strengths in the threshold region (K. Aggarwal 2001, private communication), not available in the original publication,

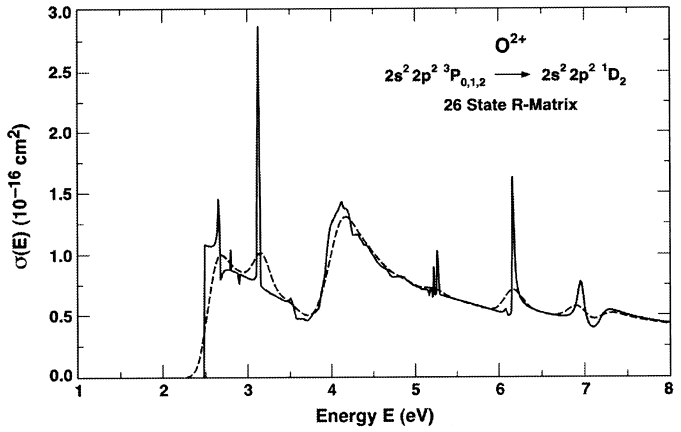

FIG. 1.—Results of calculations in the 26 state ***R***-matrix theory for the combined $2s^2 2p^2\ ^3P_{0,1,2} \rightarrow 2s^2 2p^2\ ^1D_2$ spin-forbidden transitions in O^{2+} (Aggarwal & Keenan 1999). The solid line is the unconvoluted theoretical result. The dashed line is the theoretical result convoluted with an energy-dependent width given by eq. (3) and $\Delta E_e = 0.100$ eV.

were multiplied by the degeneracy of the ground state $\omega_g = (2S_g + 1)(2L_g + 1) = 9$ to obtain the $\sigma(E)$ in Figure 1. It is clear that the excitation cross sections for this optically forbidden transition are dominated by a large number of extremely sharp resonances, most of them having widths smaller than the resolution limit of the present experiment (0.100 eV, 7.35×10^{-3} Ry). In order to compare experiment and calculation on an equal resolution footing, the data of Figure 1 were convoluted with an energy-dependent width ΔE in the CM frame given by (Smith et al. 2000)

$$\Delta E = \Delta E_e \left[1 - \left(\frac{m_e}{m_i} \right)^{1/2} \left(\frac{E_i}{E_e} \right)^{1/2} \cos \vartheta \right]. \qquad (2)$$

Here ΔE_e is the electron energy width (FWHM) in the laboratory (LAB) frame, m_e and m_i are the electron and ion masses, E_e and E_i are the electron and ion LAB energies, and ϑ is the LAB angle between the merged electron and ion beams (hence $\vartheta \approx 0°$ here). Using values appropriate for $^{16}O^{2+}$ one obtains the CM width ΔE as a function of LAB width ΔE_e by

$$\Delta E = \Delta E_e \left[1 - 5.8343 \times 10^{-3} \left(\frac{E_i}{E_e} \right)^{1/2} \right]. \qquad (3)$$

The widths from equation (3) were calculated for $\Delta E_e = 0.100$ eV and an ion-beam energy $E_i = 12.8$ keV. Results of this energy-dependent convolution are shown as the dashed line in Figures 1 and 2. One sees that evidence for the sharp resonances remains in the convoluted spectra, giving rise to broad peaks at 2.7, 3.1, and 4.2 eV. Experimental results along with the convoluted 26 state ***R***-matrix results are shown in Figure 2. These latter data were plotted as a band, to represent a "theoretical accuracy" of 5% to account for the neglect of relativistic corrections in the ***R***-matrix theory (K. Aggarwal 2001, private communication). The total error in the experimental measurements (18%) at each energy is shown at the 1.7 σ (90%) confidence level. The components of this error (e.g., counting statistics, measurement of the form factor, correction for the overlapping elastic contribution) are the same as given in Table 1 of Smith et al. (2000). The error in measurements below threshold is a conservative estimate of the error encountered in subtracting a small elastic contribution to the total scattering.

TABLE 1

EXPERIMENTAL CROSS SECTIONS $\sigma(E)$ AND COLLISION STRENGTHS $\Omega(E)$ FOR THE COMBINED $2s^2 2p^2\ ^3P_{0,1,2} \rightarrow 2s^2 2p^2\ ^1D_2$ SPIN-FORBIDDEN TRANSITIONS IN O^{2+}

Energy E (eV)	Experimental $\sigma(E)$ (10^{-16} cm^2)	Experimental Collision Strength $\Omega(E)$ (Dimensionless)
1.80.....	0.00	0.01
2.00.....	0.07	0.10
2.25.....	0.01	0.02
2.48.....	0.14	0.27
2.58.....	0.22	0.42
2.65.....	0.81	1.60
2.70.....	1.19	2.42
2.76.....	0.90	1.87
2.80.....	1.04	2.19
2.84.....	0.67	1.42
2.90.....	0.77	1.67
3.00.....	0.70	1.58
3.16.....	0.66	1.57
3.24.....	0.64	1.56
3.30.....	0.53	1.31
3.48.....	0.47	1.23
3.50.....	0.40	1.04
3.57.....	0.46	1.24
3.64.....	0.47	1.30
3.74.....	0.60	1.67
3.81.....	0.44	1.26
3.91.....	0.73	2.13
4.00.....	1.04	3.13
4.08.....	1.43	4.39
4.30.....	0.95	3.08
4.39.....	1.48	4.89
4.42.....	0.96	3.20
4.53.....	0.73	2.49
4.80.....	1.05	3.79
5.00.....	0.69	2.59
5.17.....	0.67	2.62
5.35.....	0.63	2.54

NOTE.—Nonzero values below threshold include effects of the electron-energy spread in the experiment.

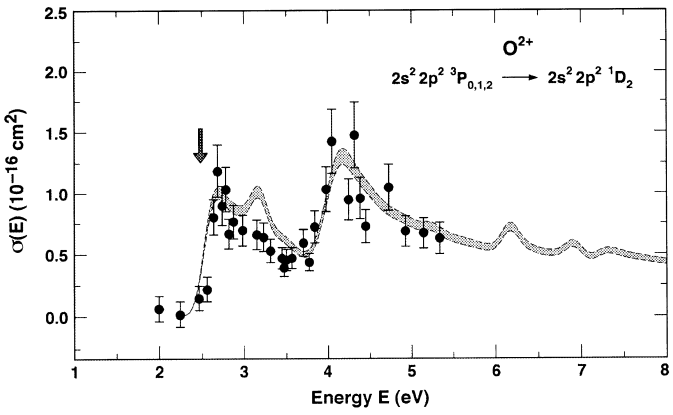

FIG. 2.—Comparison of present, experimental absolute excitation cross sections for the $2s^2 2p^2\ ^3P_{0,1,2} \rightarrow 2s^2 2p^2\ ^1D_2$ transitions in O^{2+} (*solid circles*), with theoretical results in the 26 state ***R***-matrix calculation (Aggarwal & Keenan 1999). The sharp resonance structures in the calculation have been convoluted with an energy-dependent resolution, as given by experimental conditions and eq. (3). These results are drawn with a 5% "theoretical accuracy" error band. Experimental error limits are shown at the 1.7 σ (90%) confidence level. The arrow indicates the energy threshold of this transition.

Present, measured absolute excitation cross sections for the $2s^2 2p^2\ ^3P_{0,1,2} \rightarrow 2s^2 2p^2\ ^1D_2$ spin- and symmetry-forbidden transitions in O^{2+} are listed in Table 1 at the discrete energies of the experiments and are shown in Figure 2. Each entry in Table 1 is an average of 1–3 measurements at the energy listed.

Also, for convenience in solar- and stellar-modeling calculations and for further comparison with theory, the experimental cross sections have been converted to collision strengths $\Omega(E)$, and these are listed in the third column of Table 1.

Strong resonance enhancement near threshold is clearly seen in the calculations and experimental data of Figure 2. The experimental peak at 2.7 eV is the result of the lowest-energy resonance; and the slow drop-off to 3.6 eV could arise from the sharp resonance at 3.1 eV. Evidence for the calculated resonances near 4.2 eV is clearly seen in the experiment, with the cross section increasing from 0.439×10^{-16} to 1.48×10^{-16} cm^2 between $E = 3.81$ and 4.39 eV. The highest energy of the experiments (5.35 eV) was limited by the increasing ratio of admixed elastically scattered electron signal to the inelastically scattered electron signal. This ratio was in the range 6%–30% at 5.35 eV, depending on tuning conditions. Hence, the weaker resonance structures near 6.1 and 6.9 eV could not be explored.

In conclusion, absolute experimental excitation cross sections for the spin-forbidden $2s^2 2p^2\ ^3P_{0,1,2} \rightarrow 2s^2 2p^2\ ^1D_2$ transitions in O^{2+} are presented at excitation energies from threshold of 2.48 eV to a maximum energy of 5.35 eV (or 2.2 × threshold). There is agreement with some predictions of the 26 state ***R***-matrix calculation which indicates a rich resonance structure throughout this energy range. Experiment confirms the resonance enhancements near 2.7 and 4.2 eV with its electron energy resolution of only $\Delta E_e = 0.10$ eV. Experiment does not confirm the narrow, sharp resonance near 3.1 eV (Fig. 1). This could result from the fact that the calculated resonance is weaker or narrower (or both) than shown in Figure 1, and hence is missed by experiment at its resolution.

These measurements are part of a series aimed at understanding optical emissions and energy balance in the Io torus, diffuse nebulae-H II regions, and planetary nebulae. The experiments also lend reliability to the use of the ***R***-matrix approach in calculating cross sections for those transitions which have not been measured, or which may be difficult to measure due to experimental resolution limitations.

We thank K. Aggarwal for helpful discussions and for providing results of calculations in a fine energy grid. M. Niimura thanks the National Research Council for a senior fellowship through the NASA-NRC program. This work was carried out at the Jet Propulsion Laboratory, California Institute of Technology, and was supported by the National Aeronautics and Space Administration.

REFERENCES

Aggarwal, K. M. 1993, ApJS, 85, 197
Aggarwal, K. M., & Keenan, F. P. 1999, ApJS, 123, 311
Bashkin, S., & Stoner, J. O., Jr. 1975, Atomic Energy Levels and Grotrian Diagrams (New York: Elsevier), 176
Beer, S. H., & Vaughan, A. E. 1999, Publ. Astron. Soc. Australia, 16, 134
Chutjian, A., Greenwood, J. B., & Smith, S. J. 1999, in Applications of Accelerators in Research and Industry, ed. J. L. Duggan & I. L. Morgan (New York: AIP), 881
Clementi E., & Roetti, C. 1974, At. Data Nucl. Data Tables, 14, 177
Crawford, F. L., Keenan, F. P., Aggarwal, K. M., Wickstead, A. W., Aller, L. H., & Feibelman, W. A. 2000, A&A, 362, 730
Doschek, E. E., Laming, J. M., Doschek, G. A., Feldman, U., & Wilhelm, K. 1999, ApJ, 518, 909
Gorny, S. K., Schwarz, H. E., Corradi, R. L. M., & Winckel, H. 1999, A&AS, 136, 145
Greenwood, J. B., Chutjian, A., & Smith, S. J. 2000, ApJ, 529, 605
Greenwood, J. B., Smith, S. J., Chutjian, A., & Pollack, E. 1999, Phys. Rev. A, 59, 1348
Herbert, F., & Hall, D. T. 1998, J. Geophys. Res., 103, 19915
Hibbert, A. 1975, Comput. Phys. Commun., 9, 141
Küppers, M., & Jockers, K. 1997, Icarus, 129, 48
Lozano, J. A., Niimura, M., Smith, S. J., Chutjian, A., & Tayal, S. S. 2001, Phys. Rev. A, 63, 042713 (2001)
Pilyugin, L. S. 2000, A&A, 362, 325
Smith, S. J., Greenwood, J. B., Chutjian, A., & Tayal, S. S. 2000, ApJ, 541, 501
Smith, S. J., Zuo, M., Chutjian, A., Tayal, S. S., & Williams, I. D. 1996, ApJ, 463, 808